Published in final edited form as:
J Neurosci Methods. 2009 October 30; 184(1): 124–128. doi:10.1016/j.jneumeth.2009.07.028.

Quantifying Perivascular Sympathetic Innervation: Regional Differences in Male C57BL/6 Mice at 3 and 20 Months

Jennifer B. Long[1,2] and **Steven S. Segal**[1,2,3,4]

[1]The John B. Pierce Laboratory, New Haven, Connecticut

[2]Department of Cellular and Molecular Physiology, Yale University School of Medicine, New Haven, Connecticut

[3]Department of Medical Pharmacology and Physiology, University of Missouri, Columbia, Missouri

[4]Dalton Cardiovascular Research Center, Columbia, Missouri

Abstract

Perivascular sympathetic innervation density (PSID) is a key determinant of vasomotor responses to sympathetic nerve activity. However, total axonal length (for *en passant* neurotransmission) per vessel surface area has not been well defined, particularly while preserving 3-dimensional vascular structure. We developed a novel method for quantifying PSID using 3-dimensional anatomical reconstruction and compare a variety of blood vessels in Young (3 months) and Old (20 months) male C57BL/6 mice. Individual vessels were dissected and immunolabeled for tyrosine hydroxylase. The total length of fluorescent axons in defined vessel surface areas was quantified by mapping Z-stack images (magnification = 760×). For young mice, innervation densities (μm axon length/μm^2 vessel surface area) in mesenteric (0.075 ± 0.002) and femoral (0.080 ± 0.003) arteries were greater ($P<0.05$) than mesenteric veins (0.052 ± 0.002) and gracilis muscle feed arteries (0.040 ± 0.002). Carotid arteries and gracilis muscle veins were not immunoreactive nor were there significant differences in PSID between Young and Old animals. We demonstrate a novel approach to quantify sympathetic innervation of the vasculature while preserving its 3-dimensional structure and document regional variation in PSID that persists with aging in mice. This analytical approach may used for quantifying PSID in other tissues that have superficial vessels which can be studied *in situ* or from which embedded vessels can be excised. With appropriate visualization of neuronal projections, it may also be applied to tissues that have other sources of superficial innervation.

Keywords

catecholamines; perivascular innervation; sympathetic nerves; 3-dimensional mapping

Introduction

Sympathetic innervation of the peripheral vasculature is integral to the distribution of cardiac output and the regulation of systemic blood pressure. Postganglionic sympathetic nerves follow

Corresponding Author: Steven S. Segal, Ph.D., University of Missouri, Department of Medical Pharmacology and Physiology, One Hospital Drive, MA415 Medical Science Building, Columbia, MO 65212 USA, Tel: (573) 882-2553 Fax: (573) 884-4276, segalss@health.missouri.edu.

the arterial supply into tissues, course along arterioles and, in skeletal muscle, terminate prior to capillary beds (Marshall, 1982; Saltzman et al., 1992). Norepinephrine released *en passant* during the firing of sympathetic nerves promotes vasoconstriction by activating postjunctional α-adrenergic receptors on smooth muscle cells. Whereas autonomic neural control of the peripheral circulation is integral to acute cardiovascular adaptations to physical stress, enhanced activity of the sympathetic nervous system is implicated in such cardiovascular disorders as heart failure and hypertension (Augustyniak et al., 2002). As determined using microneurography and hemodynamic measurements, such undesirable conditions become more prevalent with aging, which has been associated with enhanced sympathetic nerve activity and peripheral vasoconstriction even in healthy individuals (Dinenno and Joyner, 2006). Remarkably, little is known of whether perivascular sympathetic innervation density (PSID) differs between young and old, particularly in the peripheral vasculature.

Whereas PSID is difficult to evaluate directly in human subjects, animal models permit more invasive and direct methods of quantification. Earlier anatomical studies of how aging affects sympathetic innervation have often relied on rodents as a model system while evaluating internal organs such as the spleen (Felten et al., 1987), pancreas (Lindsay et al., 2006) and heart (Bruzzone et al., 2003). In contrast, relatively little attention has been given to the peripheral vasculature, nor has there been a standardized procedure for quantifying PSID. Moreover, the preparation of tissue samples for evaluating sympathetic innervation often involves embedding and sectioning (Lindsay et al., 2006) or dehydration and heating (Bruzzone et al., 2003; Marshall, 1982; Saltzman et al., 1992). Such practices can dramatically alter tissue morphology from that which is manifested in the intact system. Remarkably, despite the increasing use of mice in experimental models, there is little quantitative information regarding PSID in the mouse. To address these limitations, we developed a method for quantifying PSID of intact vessel segments and investigated distinct regions of the vascular tree to evaluate whether the anatomical PSID differed between Young (3 month) and Old (20 month) male C57BL/6 mice.

Materials and Methods

Animal purchase and care

Experimental procedures were approved by the Institutional Animal Care and Use Committees of the John B. Pierce Laboratory and the University of Missouri and were performed in accordance with the NIH *Guide for the Care and Use of Laboratory Animals*. Male C57BL/6 mice were obtained from The Jackson Laboratory (Bar Harbor, ME) and studied when ~3 months (‘Young’, n=5; 27 ± 2 g) and ~20 months (‘Old’, n=7; 34 ± 5 g) of age. Mice were housed at 24 °C on a 12h-light/12h-dark cycle with fresh food and water provided *ad libitum*.

Vessel sampling and immunolabeling

A mouse was anesthetized with sodium pentobarbital (50 mg/kg, intraperitoneal injection). While viewing through a stereomicroscope, entire common carotid and femoral arteries, gracilis muscle feed arteries and veins of the left side were carefully excised along with second-order arteries and veins from the mesentery. Prior to removal, the dimensions of each vessel were measured *in situ* using a calibrated eyepiece reticule. The mouse was then euthanized with an overdose of anesthetic. Intact vessel segments were pinned at each end to a thin (~ 2 mm) layer of Sylgard® (#184; Dow Corning Corp., Midland, MI) in a Petri dish to approximate respective dimensions *in situ.* While viewing through the stereomicroscope, connective tissue was carefully dissected away by hand using fine forceps to grasp its edges and trimming with fine microdissection scissors. Based on our preliminary experiments, great care was taken to avoid stripping off the adventitia and possible damage to the perivascular nerves. Vessels were

fixed in 4% paraformaldehyde for 30 minutes and then incubated in 0.5% Pontamine Sky Blue (Sigma-Aldrich, St. Louis, MO) in phosphate-buffered saline (PBS) for 30 minutes to reduce background fluorescence. This was followed by 1 hour at room temperature in a blocking solution of 4% normal goat serum/0.3 % Triton X-100 in PBS, then overnight at 4 °C in blocking solution containing an affinity-purified polyclonal antibody against tyrosine hydroxylase (#AB152; rabbit anti-rat. 1:1000; Chemicon; Temecula, CA), the rate-limiting enzyme for catecholamine biosynthesis. Vessel segments were then washed in PBS and incubated for 1 hour with secondary antibody (Alexa Fluor-488 goat anti-rabbit, 1:1000; Invitrogen, Carlsbad, CA), washed again and (while remaining pinned to Sylgard) positioned on a glass slide. Preparations remained immersed in PBS during image acquisition to maintain hydration and preserve vessel morphology.

Digitized mapping of perivascular nerve fibers

Specimens were viewed along their axis (i.e., in the direction of blood flow). A well-defined segment (length, 400-600 μm) within the midregion of the vessel that contained intact axonal networks was identified. Using a NeuroLucida system (MicroBrightField; Williston, VT) integrated with a Nikon E600 fluorescent microscope, the superior half of the vessel segment was digitized to obtain the total length of nerve fibers. Image stacks were acquired in 2 μm steps through the Z-axis of the vessel (i.e., normal to the direction of blood flow) using a 20× objective (numerical aperture = 0.50) coupled to a cooled megapixel CCD camera (Optronics Microfire; Goleta, CA). Data were acquired by focusing vertically from the uppermost surface of the vessel towards the center until reaching its maximum width. The image stack was displayed on an Ultrasharp monitor at total magnification = 760×. Using a joystick controller coupled to a personal computer and interactive software (NeuroExplorer; MicroBrightField), each axonal network was mapped with a spatial resolution of ~1 μm by 'tracing' fluorescent axons throughout the stack to determine total axon length. The corresponding surface area was obtained by tracing the vessel contour and determining its major (width) and minor (depth of image stack) radii. As vessel segments were elliptical in cross section (attributable to partial collapse with loss of intravascular pressure), they were treated as ellipsoidal cylinders. Thus, surface area was calculated as equal to: $\pi L [(r_1^2 + r_2^2)/2]$, where L = segment length, r_1 = vertical depth of image stack (minor radius, see Table) and r_2 = maximum width/2 (major radius, see Table). For each vessel segment analyzed, the perivascular sympathetic innervation density was calculated: PSID = μm axon length/μm^2 vessel surface area.

Statistics

Our goal was to analyze 5 vessels of each type from respective age groups, with each vessel from a different mouse. However, because vessels from Old were more fragile than those of Young, only 3 out of 7 of the smallest vessel (gracilis muscle feed artery) were suitable for analysis. Data were analyzed using two-way analysis of variance (innervation density × age-group). When significant F-ratios were obtained, Tukey tests were performed for post-hoc comparisons. Differences were accepted as statistically significant when $P < 0.05$. Summary values (Table) are presented as means ± standard error (S.E.).

Results

As illustrated in the Figure, tyrosine hydroxylase immunolabeling revealed mesenteric and femoral arteries to be enmeshed within dense networks of sympathetic axons while mesenteric veins and gracilis feed arteries appeared less densely innervated. Quantification of innervation density (Table) confirmed significant regional variation in PSID. Respective values for mesenteric and femoral arteries were not significantly different from each other while both were significantly greater ($P < 0.05$) than mesenteric vein and gracilis feed artery. Gracilis feed arteries were less densely innervated than ($P < 0.05$) than mesenteric veins. Neither the overall

size nor the density of PSID differed significantly between Young and Old for any of the vessels examined. Carotid arteries and gracilis muscle veins were devoid of sympathetic innervation (not shown), effectively providing negative controls.

Discussion

The present findings illustrate that fluorescent immunolabeling for tyrosine hydroxylase followed by 3-dimensional mapping of anatomically-defined vessel surfaces enables reproducible quantification of the density of perivascular sympathetic nerves over curved surfaces. The consistency of values obtained with this method is illustrated by significant regional variation in the density of perivascular sympathetic innervation (Table). As little is known of how aging may influence PSID in the peripheral vasculature, we compared measurements in Young (3 month) and Old (20 month) C57BL/6 male mice because these animals exhibit alterations in blood flow control to skeletal muscle with aging (Bearden et al., 2004) that are consistent with changes observed in humans (Dinenno and Joyner, 2006).

Evaluating sympathetic innervation of the vasculature

In human subjects, the efferent activity of sympathetic nerves is routinely evaluated using microneurography in conjunction with circulating levels of norepinephrine to indicate neurotransmitter release, often while monitoring blood flow to affected limbs. Such measurements have been instrumental in establishing that impaired blood flow to skeletal muscle in older subjects is associated with enhanced sympathetic vasomotor tone (Dinenno and Joyner, 2006). As determined in rats using fluorescence histochemistry for catecholamines (with formaldehyde vapor or glyoxylic acid reaction), aging has been associated with an apparent reduction in perivascular sympathetic innervation of the heart (Bruzzone et al., 2003) and spleen (Felten et al., 1987). However there is little information with respect to how aging may affect innervation density of the peripheral vasculature, particularly in the mouse.

In light of evidence from rat spinotrapezius (Marshall, 1982) and cremaster (Fleming et al., 1987) muscle preparations and from the rat mesentery (Furness and Marshall, 1974) that sympathetic vasoconstriction is related qualitatively to the extent of perivascular innervation, the present experiments evaluated whether PSID in mice was affected by aging. Our finding that the regional variation in innervation density was not significantly different between Young and Old (Table) is consistent with functional *in vitro* studies indicating that the functional sympathetic innervation of rat femoral and renal arteries was preserved with aging (Duckles et al., 1985). Collectively, these findings indicate that changes other than the distribution of sympathetic axons over the vessel surface may contribute to enhanced sympathetic vasoconstriction with aging (Dinenno and Joyner, 2006).

The selection of vessels studied here was based upon blood flow through vessels supplying the head, gut and limbs. The lack of sympathetic innervation of the carotid artery found here in mice is consistent with earlier reports for the rat, rabbit and guinea pig (Damon, 2005; Luff and McLachlan, 1989). However, it contrasts with findings by others in the guinea pig (Cowen and Burnstock, 1980), rabbit and the cat (Knoche and Kienecker, 1977), where the carotid artery was found to be more densely innervated than the mesenteric artery and vein. Differences between studies for the same species may reflect corresponding variations in where respective vessels were sampled or how they were prepared for observation. For the present study, we sampled the midregion of the common carotid artery below its bifurcation into the internal and external branches and it is possible that these latter branches may be innervated by projections from the superior cervical ganglion en route to the cerebral circulation and other targets in the head.

Vessels supplying and draining the gracilis muscle were sampled here to represent blood flow control to skeletal muscle. While the feed artery was richly innervated, the adjacent vein was devoid of sympathetic nerves. This difference is consistent with earlier findings indicating that while resistance vessels of skeletal muscle are enmeshed with sympathetic nerves neither capillaries nor postcapillary venules are innervated (Fleming et al., 1987; Marshall, 1982; Saltzman et al., 1992). In distinct contrast from skeletal muscle vasculature, and consistent with previous observations in rats and Guinea pigs (Cowen and Burnstock, 1980; Furness and Marshall, 1974; Luff and McLachlan, 1989), veins as well as arteries of the mouse mesentery are innervated by sympathetic axons (Figure) with greater PSID in the arteries (Table).

Methodological considerations

This study is limited to a stereological analysis of vascular innervation by sympathetic adrenergic axons. Earlier studies that have evaluated sympathetic innervation have often focused on the vasculature of a single organ or vascular bed (Knoche and Kienecker, 1977; Marshall, 1982; Saltzman et al., 1992) and have relied extensively on catecholamine fluorescence (Cowen and Burnstock, 1980; Knoche and Kienecker, 1977; Marshall, 1982; Saltzman et al., 1992). However, such approaches typically dry and heat samples in order to visualize the fluorescent product. It should also be recognized that background fluorescence arising from elastic lamina can make it difficult to distinguish perivascular nerves in such preparations, particularly in vessel cross-sections (Knoche and Kienecker, 1977). While fixation and embedding can be performed before staining (Knoche and Kienecker, 1977) or tissues secured to reduce distortion during dehydration (Saltzman et al., 1992), the present experiments are the first to have maintained vessel samples fully hydrated at *in situ* length and thus in a state that more closely approximates conditions in the intact system.

The data acquisition and analysis system used in the present study was developed originally for reconstructing neuronal projections and mapping regions of the brain. Our experiments thereby represent a novel application of this methodology to enable 3-dimensional determination of innervation patterns over curved surfaces. Thus the acquisition of data through image stacks in the Z-axis uniquely enabled accounting for vessel curvature in order to accurately calculate the surface area of hydrated intact vessel segments. In turn, innervation densities expressed relative to surface area provide a standard reference across vessels of different radii (Table).

Using the same units as developed in this study for PSID, sympathetic innervation of arterioles within the rat spinotrapezius muscle (Saltzman et al., 1992) is consistent with values reported here (Table). Unlike the present study, intact muscles were dehydrated to observe perivascular catecholamine fluorescence and were analyzed in 2 dimensions (Saltzman et al., 1992). In such thin preparations, the relatively small diameter of microvessels reduces the absolute depth of curvature that was accounted for here in larger vessels by optical sectioning through the Z-axis.

Quantification of PSID in common units enables direct comparisons across studies. In contrast, earlier studies have typically described patterns of innervation (or lack thereof) that characterize particular vascular networks (Fleming et al., 1987; Marshall, 1982). Others present relative comparisons between sections taken from different regions of a particular tissue [e.g., the mouse pancreas (Lindsay et al., 2006)]. However, such approaches make it difficult to make absolute comparisons across different tissues or between species and laboratories. We suggest that axonal length per vessel surface area is a useful standard for reference while recognizing that neurotransmitters are released *en passant* from boutons positioned along the perivascular axons. While boutons were not analyzed here, such details can be incorporated by acquiring images at higher magnification for greater spatial resolution. For example, electron microscopic studies of sympathetic innervation have reported the frequency of neuromuscular

junctions per mm^2 of outer smooth muscle surface (Luff and McLachlan, 1989). Though such units differ from those applied here, they provide another standard that, consistent with the present findings, has documented rich innervation of the mesenteric artery and its absence in the carotid artery.

Conclusion

Through sampling distinct, well-defined regions of the vascular tree, the present study has provided quantitative indices of sympathetic innervation in peripheral blood vessels of the mouse. Maintaining *in situ* dimensions during histological processing and stereological measurements enabled accurate determinations of innervation densities. Our finding that regional differences were statistically significant and conserved between age-groups supports the application of this stereological approach to reproducibly quantifying PSID. The overall lack of differences in vascular innervation between Young and Old mice indicate that regional differences in sympathetic innervation remain effective during aging. This analytical approach may used for quantifying PSID in other tissues that have superficial vessels which can be studied *in situ* or from which embedded vessels can be excised. With appropriate visualization of neuronal projections, it may also be applied to tissues that have other sources of superficial innervation.

Acknowledgments

We are grateful to Dr. Torben R. Uhrenholt and Chady H. Hakim for valuable contributions and the outstanding technical support from MicroBrightField in refining NeuroExplorer software to optimize the stereological analyses used herein. This study was supported by grant RO1-HL086483 from the National Institutes of Health (NIH), United States Public Health Service. JBL was supported by NIH T32-GM07527.

References

Augustyniak RA, Tuncel M, Zhang W, Toto RD, Victor RG. Sympathetic overactivity as a cause of hypertension in chronic renal failure. J Hypertens 2002;20:3–9. [PubMed: 11791019]

Bearden SE, Payne GW, Chisty A, Segal SS. Arteriolar network architecture and vasomotor function with ageing in mouse gluteus maximus muscle. J Physiol 2004;561:535–45. [PubMed: 15388783]

Bruzzone P, Cavallotti C, Mancone M, Tranquilli Leali FM. Age-related changes in catecholaminergic nerve fibers of rat heart and coronary vessels. Gerontology 2003;49:80–5. [PubMed: 12574668]

Cowen T, Burnstock G. Quantitative analysis of the density and pattern of adrenergic innervation of blood vessels. A new method. Histochemistry 1980;66:19–34. [PubMed: 7390874]

Damon DH. Sympathetic innervation promotes vascular smooth muscle differentiation. Am J Physiol 2005;288:H2785–91.

Dinenno FA, Joyner MJ. Alpha-adrenergic control of skeletal muscle circulation at rest and during exercise in aging humans. Microcirculation 2006;13:329–41. [PubMed: 16611594]

Duckles SP, Carter BJ, Williams CL. Vascular adrenergic neuroeffector function does not decline in aged rats. Circ Res 1985;56:109–16. [PubMed: 2981645]

Felten SY, Bellinger DL, Collier TJ, Coleman PD, Felten DL. Decreased sympathetic innervation of spleen in aged Fischer 344 rats. Neurobiol Aging 1987;8:159–65. [PubMed: 3587492]

Fleming BP, Barron KW, Howes TW, Smith JK. Response of the microcirculation in rat cremaster muscle to peripheral and central sympathetic stimulation. Circ Res 1987;61:II26–31. [PubMed: 3664985]

Furness JB, Marshall JM. Correlation of the directly observed responses of mesenteric vessles of the rat to nerve stimulation and noradrenaline with the distribution of adrenergic nerves. J Physiol 1974;239:75–88. [PubMed: 4851199]

Knoche H, Kienecker EW. Sympathetic innervation of the carotid bifurcation in the rabbit and cat: blood vessels, carotid body and carotid sinus. A fluorescence and electron microscopic study. Cell Tissue Res 1977;184:103–12. [PubMed: 922856]

Lindsay TH, Halvorson KG, Peters CM, Ghilardi JR, Kuskowski MA, Wong GY, Mantyh PW. A quantitative analysis of the sensory and sympathetic innervation of the mouse pancreas. Neuroscience 2006;137:1417–26. [PubMed: 16388907]

Luff SE, McLachlan EM. Frequency of neuromuscular junctions on arteries of different dimensions in the rabbit, guinea pig and rat. Blood Vessels 1989;26:95–106. [PubMed: 2758110]

Marshall JM. The influence of the sympathetic nervous system on individual vessels of the microcirculation of skeletal muscle of the rat. J Physiol 1982;332:169–86. [PubMed: 7153926]

Saltzman D, DeLano FA, Schmid-Schonbein GW. The microvasculature in skeletal muscle. VI. Adrenergic innervation of arterioles in normotensive and spontaneously hypertensive rats. Microvasc Res 1992;44:263–73. [PubMed: 1479927]

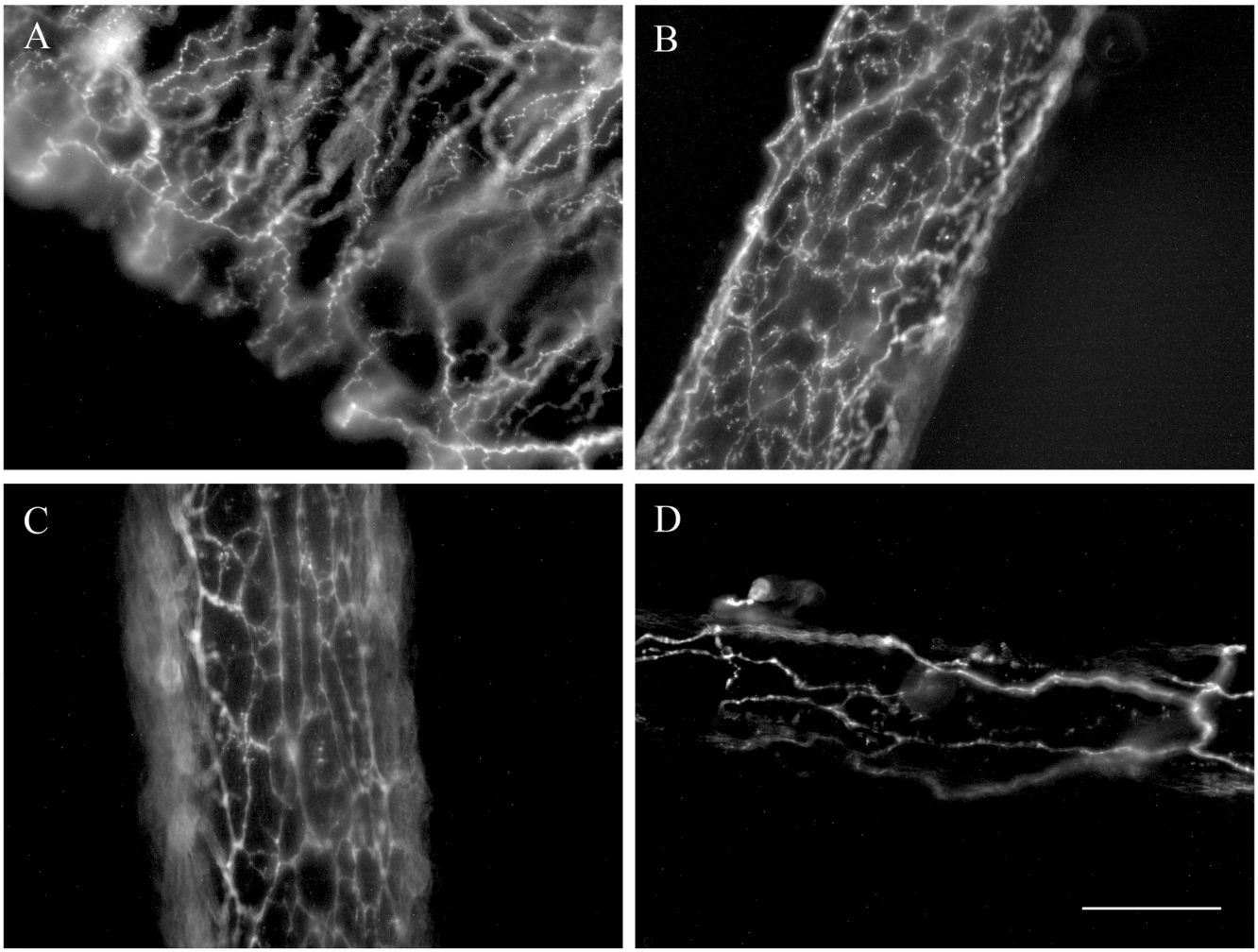

Figure. Regional perivascular sympathetic innervation

Images illustrate immunolabeling for tyrosine hydroxylase in representative vessels from Young C57BL/6 male mice. **A**: mesenteric vein; **B**: mesenteric artery; **C**: femoral artery; **D**: gracilis muscle feed artery. Each image is a 2-dimensional representation of a compressed Z-stack series (see METHODS for details). Scale bar = 100 μm and applies to all panels.

Table

Dimensions and sympathetic innervation of vessel segments

Minor and major radii, surface area, total nerve length and innervation densities for Young and Old C57BL/6 male mice. The mesenteric artery (**MA**) and femoral artery (**FA**) had the highest innervation densities and were not significantly different from each other. The mesenteric vein (**MV**) and gracilis feed artery (**GFA**) had significantly lower innervation densities (* indicates $P < 0.05$ for GFA and MV vs. MA and FA; + indicates $P < 0.05$ for GFA vs. MV). There were no significant differences in innervation densities between Young and Old age-groups for respective vessels. Summary data are means ± S.E. with n=5 for each cell except for GFA in Old, where n=3.

Vessel ID	Minor Radius (μm)		Major Radius (μm)		Surface Area ($\mu m^2 \times 10^3$)		Nerve Length ($\mu m \times 10^2$)		Innervation Density ($\mu m/\mu m^2 \times 10^{-2}$)	
	Young	Old	Young	Old	Young	Old	Young	Old	Young	Old
GFA*+	45 ± 1	41 ± 2	49 ± 3	54 ± 4	85.6 ± 3.2	78.7 ± 6.5	34.0 ± 1.4	35.7 ± 2.9	4.0 ± 0.2	4.6 ± 0.2
FA	51 ± 3	46 ± 1	79 ± 7	88 ± 5	92.6 ± 4.3	95.4 ± 4.8	72.0 ± 4.0	65.6 ± 3.1	8.0 ± 0.3	7.2 ± 0.3
MA	60 ± 3	53 ± 2	87 ± 9	99 ± 9	128.2 ± 18.8	129.5 ± 12.3	94.5 ± 11.6	91.7 ± 5.7	7.5 ± 0.2	7.1 ± 0.3
MV*	60 ± 4	53 ± 2	121 ± 10	108 ± 11	167.3 ± 20.7	151.0 ± 19.7	87.4 ± 11.8	72.5 ± 8.0	5.2 ± 0.2	5.0 ± 0.4